Available online at www.sciencedirect.com
ScienceDirect
Chemical Engineering and Processing 47 (2008) 1530–1540
Chemical Engineering and Processing Process Intensification
www.elsevier.com/locate/cep

Hydrodynamic aspects in anaerobic fluidized bed reactor modeling

Mauren Fuentes [a,b], Nicolás J. Scenna [a,c,*], Pío A. Aguirre [a,d], Miguel C. Mussati [a,c]

[a] *INGAR, Instituto de Desarrollo y Diseño (CONICET-UTN), Avellaneda 3657, (3000) Santa Fe, Argentina*
[b] *Depto de Ciencias Básicas - UTN FRSF, Lavaise 610, (3000) Santa Fe, Argentina*
[c] *CAIMI-UTN FRR, Zeballos 1341, (2000) Rosario, Argentina*
[d] *Facultad de Ing. Qca, UNL, Santiago del Estero 2829, (3000) Santa Fe, Argentina*

Received 5 July 2006; received in revised form 16 June 2007; accepted 10 July 2007
Available online 13 July 2007

Abstract

The main purpose of this paper is to analyze the adequacy of some hypotheses assumed in the literature for modeling mass transfer phenomena and hydrodynamics in bioreactors. Four different hydrodynamic models were investigated to simulate the dynamic behavior of an anaerobic fluidized bed reactor (AFBR). A total developed flow condition and the assumption of an incipient gas phase are some of the evaluated hypotheses. All AFBR models simultaneously compute the dynamics of the phases and their components, including the effect of the biofilm growth in the fluidization characteristics. From a computational point of view, ordinary and partial differential equation-based models were calculated using gPROMS (Process System Enterprise Ltd.). Simulations based on a case study were compared. The bioreactor performance was analyzed through the main variable profiles such as phase holdups and bed height, pH, chemical oxygen demand (COD), biofilm concentration and biogas flow rate. In a previous paper [M. Fuentes, M.C. Mussati, N.J. Scenna, P.A. Aguirre, Global modeling and simulation of a three-phase fluidized bed bioreactor, Comput. Chem. Eng., Ms. Ref. No.: 4281, submitted for publication], a heterogeneous model of a three-phase bioreactor system was presented by proposing a one-dimensional (axial) dispersive model. Its results are here used to establish a reference point. For example, the fact of considering a three-phase system with total developed flow (hydrodynamic pseudo-steady state) and complete mixture in all phases causes deviations around 5% in predictions of biofilm concentration, and 0.5% in predictions of liquid and gas phase component concentrations, when compared with results from the phenomenological dispersive model. However, predicted total COD removal efficiency is almost the same for both models. Although the gas holdup is negligible when compared with the liquid and solid ones in anaerobic fluidized bed reactors, results from model simplification assuming an incipient gas phase differ considerably from predictions based on original three-phase modeling.

Keywords: Hydrodynamics; Three-phase systems; Two-phase systems; Dynamic modeling and simulation; Anaerobic fluidized bed reactors

1. Introduction

The main interest of hydrodynamics modeling approach in a context of fluidized bed bioreactor modeling is to calculate the fluidization characteristics such as holdup and velocity of each phase present in the reactor, due to their influence on the system residence time, reactor size, specific biofilm superficial area, mass transfer and biofilm detachment processes. Indeed, characteristics of fluidization in a bioreactor are functions of biofilm concentration.

A biological fluidized bed reactor consists of a column containing an inert material support onto which biofilm develops to form bioparticles. Gas accumulation and particle sedimentation take place in a separation compartment placed over the column. From a hydrodynamic point of view, the treated effluent, biogas, fresh feed, and recirculation flows are the main streams to be calculated. Although both aerobic and anaerobic systems involve a gas phase, this is injected to column in aerobic reactors and is generated from degradation processes in anaerobic ones. Solid holdup varies during the biological time horizon due to the ongoing microbiological processes: growth, death, detachment and hydrolysis of biomass. Gas holdup also varies but its contribution is generally negligible compared to the solid and liquid holdups in anaerobic reactors. Even when these microbiological processes cause a time variation of bed porosity, this change is sufficiently

* Corresponding author. Tel.: +54 342 4534451; fax: +54 342 4553439.
E-mail addresses: mfuentes@ceride.gov.ar (M. Fuentes), nscenna@ceride.gov.ar (N.J. Scenna), paguir@ceride.gov.ar (P.A. Aguirre), mmussati@ceride.gov.ar (M.C. Mussati).

0255-2701/$ – see front matter © 2007 Elsevier B.V. All rights reserved.
doi:10.1016/j.cep.2007.07.001

slow compared to those caused by a hydrodynamic transient [1,2].

The application of empirical or semi-empirical models to predict hydrodynamics of fluidized beds requires estimating the phase holdups and/or superficial velocities. These models consider a steady state or total developed flow condition. The fact that bioparticles properties vary during the biological transient causes a hydrodynamic pseudo-steady state condition. A phenomenological model based on mass and momentum balances allows the simultaneous prediction of the dynamics of the phases and their components, including the effect of the biofilm growth in the fluidization characteristics and interaction among them in both hydrodynamic and biological transients [1,2].

Most published models oriented to calculate the bioreactor hydrodynamics [3–6] do not consider the mass transfer through the interfaces. In a previous paper, Fuentes et al. [1] described all terms that compute the mass transfer in the phases and interfaces of the bioreactor system. Authors proposed a heterogeneous model of a three-phase solid–liquid–gas system to investigate the hydrodynamics and biological behavior and the system performance of anaerobic fluidized bed reactors (AFBRs) for treating wastewaters. Global modeling of AFBRs involved differential mass and momentum balance equations for the three phases, differential mass balance equations for phase components, and other algebraic equations to compute the biochemical and physico-chemical processes [1,2]. These processes were described using the Anaerobic Digestion Model No. 1 (ADM1) of the *International Water Association IWA* [7]. A one-dimensional (1D axial) dynamic model was proposed and different flow patterns for the phases were analyzed. The AFBR model allows to calculate variation of properties along the axial direction of the bed, including bed stratification and changes in the particle characteristics (density and diameter). Bioreactor performance was analyzed through the main variable profiles such as phase holdup and velocity, pH, biomass concentration and generated biogas flow. Depending on phase dispersion coefficient values, i.e. different flow conditions, different biomass concentration profiles were obtained along the axial direction of the bed. The effect of the support particle characteristics (particle density and diameter) on the biofilm processes and bed fluidization was studied. As shown, an increase in the particle diameter or density requires an increase in the fluid velocity at the reactor inlet to maintain equal initial fluidization characteristics. Therefore, lower attached biomass concentration values and, thus, different stratification levels were predicted during the biological transient. The mathematical model was implemented and solved using the process modeling software tool general PROcess Modeling System (gPROMS; Process Systems Enterprise Ltd. [8,9]). It facilitates mathematical analysis taking into account different hypotheses related to phase modeling and hydrodynamics. In fact, each new assumption determines the nature of a new modeling approach. While that paper was oriented to present the bioreactor model focused on coupling the anaerobic biofilm processes and hydrodynamics, and evaluating bed stratification, the present work is mainly focused on simulation-based analysis of results from four different hydrodynamic models. Model assumptions on mass transfer and hydrodynamics are described in the corresponding sections. In order to establish a workable point of comparison among all reactor models, results presented by Fuentes et al. [1] for a total developed flow condition (see Section 3) were included.

The paper is organized as follows: in Section 2, main equations and sensitivity analysis of model parameters to describe the hydrodynamic subsystem in four AFBR models are presented. Simulation results for a case study using these models are compared in Section 3. Computational and numerical aspects of model solution using gPROMS are described in Section 4; and finally, conclusions are drawn in Section 5.

2. Hydrodynamic models

For all modeling approaches, biochemical transformations are assumed to occur only in the fluidized bed zone but not in the free-support material zone. No mass transfer limitations in the biofilm and liquid film are assumed. The substrate concentration has the same value throughout the biofilm. This behavior is commonly observed in anaerobic biofilms of thin thickness [2].

Homogeneous biofilm distribution on the support particles, constant density and diameter of the support particles, constant wet biofilm density and spherical geometry are assumed for the bioparticle model (see Eqs. (5)–(7)). The number of support particles (i.e. the number of bioparticles) is assumed constant and these are homogeneously distributed within the entire reactor. These simplifying assumptions were introduced to make the model workable, although they do not completely reflect reality. Extension of these assumptions to more realistic conditions (e.g. introduction of the size distribution of particles, variable density of biofilm with time) will be the next step in the development of this modeling concept.

The heterogeneous and dynamic model of a three-phase solid–liquid–gas system proposed by Fuentes et al. [1] is considered as Model I for fluidized bed hydrodynamics modeling.

A second model (Model II) is derived by assuming a total developed flow condition and a complete mixture behavior for all phases. Semi-empirical equations are used to compute the phase fluidization characteristics (Section 2.1).

Models III and IV are based on the above ones, but considering a two-phase solid–liquid system and assuming that the formation of the gas phase has little effect on the hydrodynamic behavior [3,10–13]. In these models, constant holdup (lower than 1%) for the gas phase is assumed. Thus, mathematical expressions to calculate hydrodynamics are only applied to (solid–liquid) two-phase pseudo-system. Fig. 1 summarizes the four modeling approaches.

2.1. Main mathematical model equations

Model I is based on partial differential equation (PDE) for solving the phase mass and momentum balances and mass balances of phase components (Table 1). Although this has been named as a "phenomenological" modeling approach, empirical relationships are involved through the interaction force (F_I)

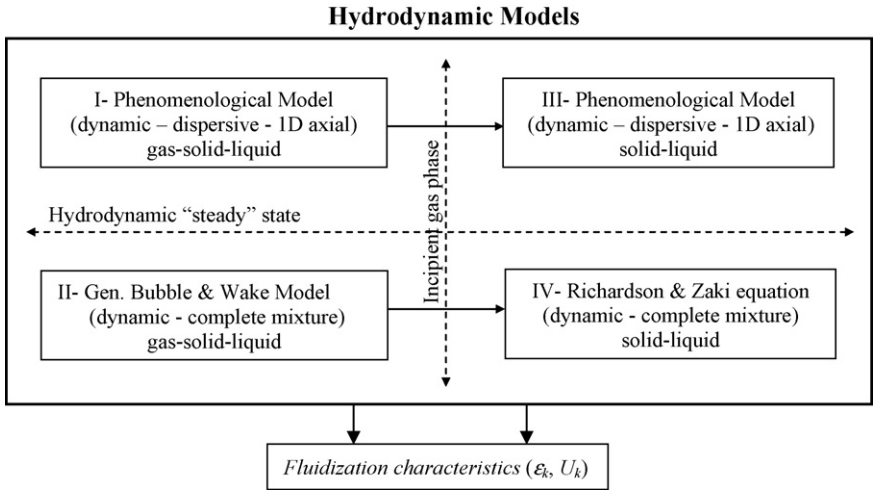

Fig. 1. Models for calculating the bioreactor hydrodynamics.

equations (see Section 2.2). Table 1 summarizes the main mathematical expressions for Model I.

The phase components are active and non-active biological species in the solid and liquid phases, soluble and insoluble chemical species, particulate material and gas phase components. All terms ($\sum_j R_{ik}^j + \sum_j T_{ik}^j$) related with mass transfer processes, model parameters and constants, and initial and boundary conditions to solve differential equations are described in Fuentes et al. [1] and Fuentes [2]. However, the main rate expressions have been summarized in Table A.1 of Appendix A.

Although support particles are homogeneously distributed, the biofilm thickness (δ), and thus, the bioparticle diameter vary with time and in the axial direction of the bed. Since the solid holdup $\varepsilon_S(z,t)$ can be interpreted as the volume fraction of the total bioparticle volume in the volume $dV = A_c dz$; from an overall material balance in the reactor unit, the height (H) of the fluidized bed is calculated as follows:

$$H = \frac{1}{A_c}\frac{N_{bp}\bar{V}_{bp}}{\bar{\varepsilon}_S} = \frac{1}{A_c}\frac{N_{bp}[1/H\int_z V_{bp}dz]}{[1/H\int_z \varepsilon_S dz]} \quad (1)$$

where V_{bp} and N_{bp} are the bioparticle volume ($V_{bp} = \pi(d_p + 2\delta)^3/6$) and the number of bioparticles ($N_{bp} = W/\rho_p V_p = W/\rho_p(\pi d_p^3/6)$), respectively.

There are several empirical and semi-empirical models to predict hydrodynamics of three-phase systems [14]. Here, the generalized bubble and wake model (GBWM) [15] is selected to describe the three-phase system in Model II. The wake concept considers the three-phase fluidized bed to be composed of: (1) the gas bubble region, (2) the wake region, and (3) the solid–liquid fluidization region. The porosity in the solid–liquid fluidization region can be expressed by the Richardson and Zaki [16] equation ($\varepsilon^n = U_l/U_t$), the wake region moves at the same velocity as the bubble, and the porosity of this region can be different as the solid–liquid fluidization one. The simplified wake theory (i.e. the liquid wakes are particle-free) [17,18] is used here to calculate the liquid holdup. The empirical equation proposed by Chern et al. [18–20] for calculating the gas holdup directly from flow velocities and solid holdup is here used. Parameter k from GBWM, which describes the relationship between volumetric fractions of wake and bubbles, is calculated using the expression proposed by Yu and Rittmann [18]. Main equations for Model II are described in Table 2. Note that terms

Table 1
Mathematical expressions for Model I [1,2]

Model I:

Phase mass balance equation

$$\partial\frac{\varepsilon_k\rho_k}{\partial t} = -\partial\frac{\varepsilon_k\rho_k U_k}{\partial z} + \frac{\partial}{\partial z}\left(D_{zk}\partial\frac{\varepsilon_k\rho_k}{\partial z}\right) + \sum_{i,j} T_{ik}$$

Phase momentum balance equation

$$\partial\frac{\varepsilon_k\rho_k U_k}{\partial t} = -\partial\frac{\varepsilon_k\rho_k U_k^2}{\partial z} + \frac{\partial}{\partial z}\left(D_{zk}\partial\frac{\varepsilon_k\rho_k U_k}{\partial z}\right) + F_{gk} + F_{pk} + F_{Ik}$$

Phase component mass balance equation

$$\partial\frac{\varepsilon_k\phi_{ik}}{\partial t} = -\partial\frac{\varepsilon_k\phi_{ik}U_k}{\partial z} + \frac{\partial}{\partial z}\left(D_k\partial\frac{\varepsilon_k\phi_{ik}}{\partial z}\right) + \sum_j R_{ik}^j + \sum_j T_{ik}^j$$

Force expressions

$$F_{gk} = -\varepsilon_k\rho_k g, \quad k = S, L, G$$

$$F_{pk} = -\varepsilon_k\frac{\partial p}{\partial z}, \quad \frac{\partial p}{\partial z} = -g\sum_k \varepsilon_k\rho_k, \quad k = S, L, G$$

$$F_{I_{S\text{-}L}} = -F_{I_{L\text{-}S}} = \xi_S(\rho_p - \rho_L)g\left(\frac{U_0 - U_S}{U_t}\right)^{4.8/n}\xi_L^{-3.8}$$

$$F_{I_{L\text{-}G}} = -F_{I_{G\text{-}L}} = \frac{36\xi_G\mu_L(U_G - U_L)}{d_B^2}$$

$$F_{E_S} = -3.2 d_{bp} g\xi_S(\rho_S - \rho_L)\frac{\partial\xi_S}{\partial z}$$

Table 2
Mathematical expressions for Model II [2]

Model II:	
Liquid phase	
Holdup	$\varepsilon_L = \left[\frac{U_l}{U_t} - k\frac{U_g}{U_t}\right]^{1/n} [1-\varepsilon_G - k\varepsilon_G]^{1-1/n} + k\varepsilon_G, \quad k = 3.5\varepsilon_L^3 \exp(-5.08\varepsilon_G)$
Velocity	$U_0 = U_l + U_g = \varepsilon_L U_L + \varepsilon_G U_G$
Phase component mass balance eq.	$A_c d\frac{\varepsilon_L \phi_{iL} H}{dt} = Q_{l_{in}}\phi^*_{iL} - Q_{l_{out}}\phi_{iL} + V\left(\sum_j R^j_{iL} + \sum_j T^j_{iL}\right),$ $\phi^*_{iL} = \frac{1}{A_c U_0}\left[Q_f \phi_{iL_f} + Q_r \phi_{iL_{z=H}}\right], Q_{l_{in}} = Q_o = U_o A_c, Q_{l_{out}} = U_l A_c$
Solid phase	
Holdup	$\varepsilon_S + \varepsilon_L + \varepsilon_G = 1$
Velocity	$U_S = 0$
Phase component mass balance eq.	$A_c d\frac{\varepsilon_S \phi_{iS} H}{dt} = V\left(\sum_j R^j_{iS} + \sum_j T^j_{iS}\right)$
Gas phase	
Holdup	$\frac{U_g}{\varepsilon_G} = \frac{U_g}{1-\varepsilon_S} + \frac{U_l}{1-\varepsilon_S} + 0.1016 + 1.488\left(\frac{U_g}{1-\varepsilon_S}\right)^{0.5}$
Velocity	$U_g = \frac{Q_{g_{out}}}{A_c} = -\frac{d\varepsilon_G H}{dt} + \frac{V}{A_c \rho_G}\sum_{i,j} T^j_{iG}$
Phase component mass balance eq.	$A_c d\frac{\varepsilon_G \phi_{iG} H}{dt} = -Q_{g_{out}}\phi_{iG} + V\left(\sum_j R^j_{iG} + \sum_j T^j_{iG}\right)$

($\sum_j R^j_{ik} + \sum_j T^j_{ik}$) related with mass transfer processes are the same as in Model I (see Table A.1, Appendix A).

As described above, the fact of applicating empirical equations to calculate phase holdups requires estimating the liquid (U_l) and gas (U_g) phase superficial velocities. A constant volumetric flow through the fluidized bed is assumed, the velocity in the bed cross-section is equal to fluid velocity at the reactor inlet U_0 (Table 2). The generated gas is assumed to be separated from the multiphase stream in the upper part of the reactor column, and thus, the gas phase flow rate at the reactor inlet ($Q_{g_{in}}$) is equal to zero.

The largest changes on the hydrodynamic properties evidently occur during the hydrodynamic transient, and the solid phase velocity is almost zero when the fluidized bed reaches the hydrodynamic steady state [1,2]. In Model II, hydrodynamic equilibrium for bioparticles is assumed and thus, solid phase velocity is considered equal to zero ($U_S = 0$). Since the solid is confined in the control volume, no flux conditions at the reactor inlet and outlet are assumed ($Q_{s_{in}} = Q_{s_{out}} = 0$).

Similar to Eq. (1), for a complete mixture flow, i.e. when the properties are only time functions, the height of the fluidized bed is calculated as:

$$H = \frac{1}{A_c}\frac{(W/\rho_p)(1+2\delta/d_p)^3}{\varepsilon_S} \tag{2}$$

2.1.1. Simplified models (III and IV) based on the hypothesis of an incipient gas phase

For describing Models III and IV, mathematical expressions summarized in Tables 1 and 2 are only applied to solid–liquid two-phase pseudo-system, respectively. The relationship $\varepsilon_L + \varepsilon_S = 1 - \varepsilon_G = \varepsilon'$ is assumed, so that ε' is a constant value near to 1.

For these models, gas phase mass balance is reduced to calculate the generated gas flow rate ($Q_{g_{out}}$) at the reactor outlet. Specifically, for Model III the gas phase mass balance is expressed as:

$$\varepsilon_G A_c \frac{dH}{dt} = -Q_{g_{out}} + \frac{V}{\rho_G}\left[\frac{1}{H}\int_z \sum_{i,j} T^j_{iG} dz\right] \tag{3}$$

In Eq. (3), the term in brackets represents the mean value of mass transfer at the liquid–gas interface along the bed axial direction.

Interaction force ($F_{L\text{-}G}$) between liquid and gas phases is considered equal to zero when the momentun balance equation (Table 1) is applied to liquid phase in Model III.

When there is no gas flow ($\varepsilon_G = 0$) in the fluidized bed, equation to calculate liquid holdup in Model II (Table 2) becomes in the relationship for two-phase solid–liquid fluidized beds [16]. It is the main assumption used to calculate the liquid holdup in Model IV. As a constant gas phase holdup (ε_G) is considered, equation written in Table 2 to calculate ε_G is not used.

Model equations show that to predict fluidization characteristics, for three-phase or two-phase (phenomenological and empirical) modeling approaches, several important parameters, such as the terminal settling velocity of particles U_t and the bed expansion coefficient n, must be accurately determined (Tables 1 and 2). The sensitivity analysis presented in Section 2.2 is not intended to be a review of correlations for estimation

Table 3
Correlations for calculating parameters n and C_D

Richardson and Zaki [16]
$n = 4.4Re_t^{-0.1}$, $1 < Re_t < 500$; $C_D = 18.5Re_t^{-0.6}$, $0.3 < Re_t < 1000$[a]
Hermanowicz and Ganzarczyk [21]
$n = 10.35Re_t^{-0.18}$, $n = 10.35Re_t^{-0.18}$; $C_D = 17.1Re_t^{-0.47}$, $40 < Re_t < 81$
Thomas and Yates [25][b]
$n = 30.0Re_t^{-0.505}$, $40 < Re_t < 81$; $C_D = 17.1Re_t^{-0.47}$, $40 < Re_t < 81$
Mulcahy and Shieh [22]
$n = 10.35Re_t^{-0.18}$, $40 < Re_t < 90$; $C_D = 36.6Re_t^{-0.67}$, $40 < Re_t < 90$
Yu and Rittmann [18]
$n = 4.526Re_t^{0.0126}$; $C_D = \frac{24}{Re_t} + 14.55Re_t^{-0.48}$, $40 < Re_t < 90$

[a] Suggested by Perry and Chilton [27] for smooth rigid spheres.
[b] Authors suggested the equation reported by Shieh and Chen [28] to calculate the expansion coefficient n.

of U_t and n. The aim here is to show the results dispersion using some of most cited and used correlations in literature related to biofilm reactor modeling. It should be noticed that there are new correlations recently published for the estimation of such parameters.

2.2. Sensitivity analysis of parameters U_t and n

In fluidized bed bioreactors, parameters U_t and n are functions of biofilm thickness (δ). Authors [18,21–25] have studied the effects of biofilm accumulation on these parameters in fluidized bed reactors. Table 3 summarizes some correlations to calculate n and the drag coefficient C_D, which is substituted in equation (4) to calculate U_t.

$$U_t = \left[\frac{4gd_{bp}(\rho_S - \rho_L)}{3C_D\rho_L}\right]^{0.5} \quad (4)$$

An increase in the bioparticle volume (due to a biofilm volume increase) causes a variation of bioparticle diameter d_{bp} and density ρ_{bp} (equal to the solid phase density ρ_S). From model assumptions, d_{bp} and ρ_{bp} can be calculated as:

$$d_{bp} = d_p + 2\delta \quad (5)$$

$$\rho_{bp} = \frac{\rho_p + x\rho_F}{1 + x} \quad (6)$$

where x is the volumetric ratio between biofilm and material support:

$$x = \left(\frac{d_{bp}}{d_p}\right)^3 - 1 \quad (7)$$

In Table 3, the terminal Reynolds number (Re_t) is calculated as:

$$Re_t = \frac{U_t d_{bp}\rho_L}{\mu_L} \quad (8)$$

Better agreement between experimental and predicted hydrodynamic values was obtained using the correlation proposed by Foscolo et al. [26] (Eq. (9)), even when it was not deduced to describe the hydrodynamics of AFBRs [10].

$$U_t = \frac{-17.3\mu_L + [299.29\mu_L^2 + 1.344gd_{bp}^3\rho_L(\rho_S - \rho_L)]^{0.5}}{0.672d_{bp}\rho_L}, \quad 0.2 < Re_t < 500 \quad (9)$$

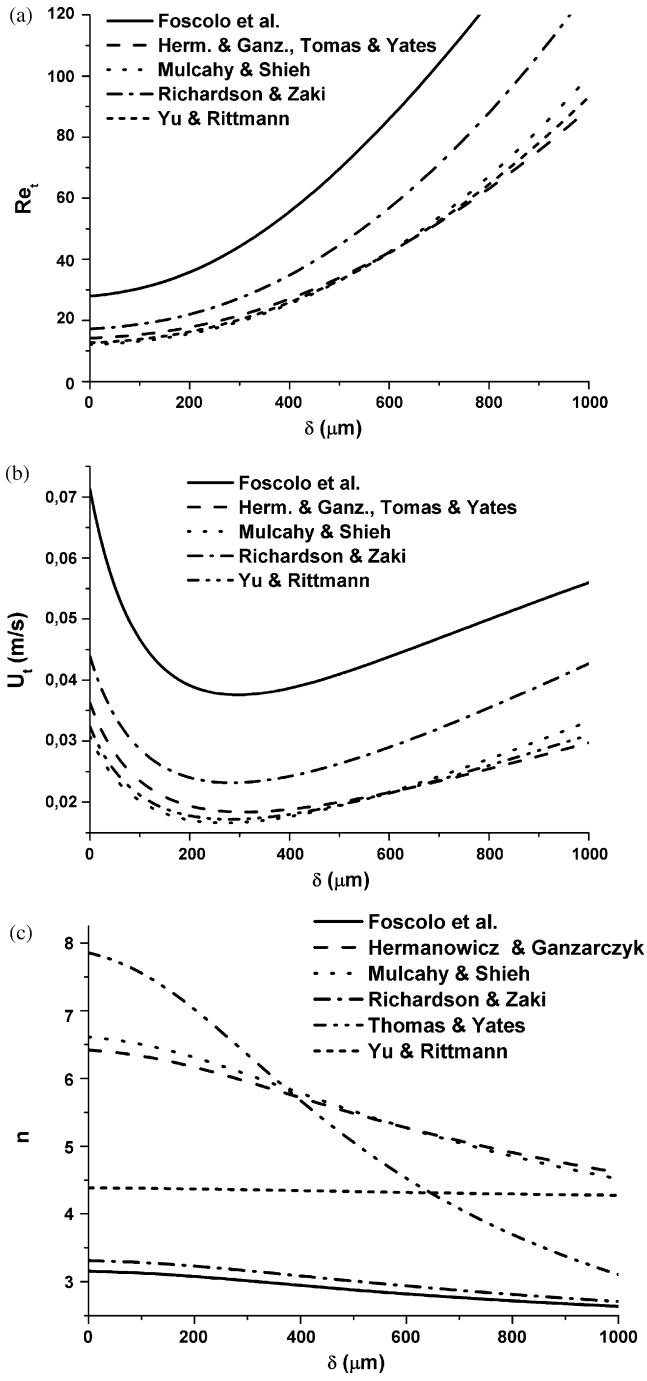

Fig. 2. Sensitivity analysis: (a) terminal Reynolds number (Re_t), (b) terminal settling velocity (U_t), and (c) bed expansion coefficient (n), as functions of biofilm thickness (δ).

Fig. 2a–c show sensitivity analysis of parameters Re_t, U_t and n, respectively, in relation to biofilm thickness (δ) using the correlations summarized in Table 3. Results from combining the

Richardson and Zaki [16] equation to calculate n (Table 3), and equation (9) to calculate U_t are added. Characteristics of support particles described in the original case study from Fuentes et al. [1] are here used; a particle diameter d_p equal to 0.35 mm and a density ρ_p of 2630 kg m^{-3} are considered. The liquid phase has been assumed as water at 35 °C ($\rho_L = 993$ kg m^{-3}, $\mu_L = 7.6 \times 10^{-4}$ kg m^{-1} s^{-1}).

For the case study (at constant d_p and ρ_p), for all correlations and as shown in Fig. 2b, terminal settling velocity increase with the biofilm thickness when it has reached values higher than 250 μm.

From Fig. 2, the biofilm thickness has to be above 600 μm for successfully applying the Hermanowicz and Ganzarczyk [21], Thomas and Yates [25], Mulcahy and Shieh [22], and Yu and Rittmann [18] correlations, which are valid for $40 < Re_t < 90$. These equations have been obtained and applied to aerobic biofilm systems in which the biofilm thickness can overshoot this value.

From the mass balance in the solid phase and the bioparticle model here assumed, the following relationship between the biofilm thickness δ and the total (active and non-active) attached biomass concentration X_T^S (see Figs. 4 and 5) can be derived:

$$X_T^S = \rho_F \left[1 - \frac{1}{(1 + 2\delta/d_p)^3} \right] \tag{10}$$

Some characteristics of support particles such as shape, roughness, and material porosity, have not yet been included in the bioparticle model. Therefore, the value of δ calculated from Eq. (10) can be interpreted as an ideal mean value. Previous experiencies showed that the biofilm is normally inhomogeneously distributed on real support particles. By scanning electron microscopy (SEM) it was observed that microorganisms are attached to approximately 50% of the superficial area of sand particles, mainly covering the deep zones of the particles due to abrasion and erosion effects on the exposed zones [29].

For the range of Re_t here investigated, original Richardson and Zaki [16] equations or their combination with the Foscolo et al. [26] equation (Eq. (9)) to calculate U_t, seem to be more appropriate to be applied to bioparticle systems with low biofilm thickness. Although no experimental data were obtained for δ, a good agreement between the predicted and experimental COD, VFA, pH, and biogas production rate values was obtained by adjustment of Model II, using well-known parameters for biochemical and physico-chemical processes, and estimating the specific biofilm detachment rate k_E for two mesophilic anaerobic lab-scale fluidized bed reactors with sand as support particles for biofilm attachment [30]. The simplified wake and bubble theory simulated successfully the main hydrodynamic events that took place in the reactors. The ω-function used for modeling the biofilm detachment rate resulted to be appropriate for representing bioreactor behavior during non-highly perturbated hydrodynamic conditions (see Appendix A). These results were obtained using the equation provided by Foscolo et al. [26] to calculate U_t and the original equation of Richardson and Zaki [16] to calculate n (Table 3). Therefore, as well as in the previous paper, these correlations are here used to calculate U_t and n.

3. Results and discussion

In this work, results of the original case study reported by Fuentes et al. [1] are used. Characteristics of support particles have been previously mentioned (Section 2.2). The reactor column has a maximum height H_{max} of 2.00 m, and a diameter D_c of 0.065 m. Support material ($W = 3.50$ kg) is loaded till reaching a static bed height H_0 of 0.70 m. 1 g of chemical oxygen demand (COD) per liter concentration of a synthetic substrate (70% glucose, 20% acetate and 10% milk powder) is fed to the bioreactor at a flow rate of 3.20 L d^{-1}. For a reactor inlet velocity U_0 of 1.81×10^{-2} m s^{-1}, a bed expansion around 45% is reached during the hydrodynamic transient.

Kim and Kim [31] equation was used to calculate the liquid phase axial dispersion coefficient:

$$\frac{d_p \varepsilon_L U_L}{D_{zL}} = 20.19 \left(\frac{d_p}{D_c} \right)^{1.66} \left(\frac{\varepsilon_L U_L}{\varepsilon_L U_L + \varepsilon_G U_G} \right)^{1.03} \tag{11}$$

A value for D_{zL} equal to 1.83×10^{-3} m^2 s^{-1} at the beginning of the biological transient is obtained, and a decrease of 0.23% is computed due to an increase of the biofilm concentration. From sensitivity analysis, values for solid and gas phase coefficients of $D_{zS} = 0.1 D_{zL}$ and $D_{zG} = 0.1 D_{zL}$, respectively, assured uniform concentration profiles (complete mixture behavior) in the solid phase [1,2]. This flow pattern was named as "totally dispersive" flow condition. Simulation results for biological transient assuming this flow condition are settled as Model I results.

Because of the low COD concentration of the reactor feed (1 g L^{-1}), expected biomass and biogas yields are too low (Fig. 4a and b). For this case study, as shown in Fuentes et al. [1], gas phase holdup presents a plug flow behavior for all tested dispersion coefficient values. Steady state values from $\varepsilon_{G(z=0)} = 0.00025$ to $\varepsilon_{G(z=H)} = 0.00047$ along the bed axial direction were obtained. These values are practically negligible when compared to liquid and solid ones. Therefore, most published works assume AFBRs as solid–liquid two-phase systems to describe their hydrodynamics. Firstly, a comparison of results considering a three-phase bioreactor system is depicted in Section 3.1. In Section 3.2, results obtained from simplified models taking into account an incipient gas phase, i.e. a two-phase solid–liquid pseudo-system, are presented.

3.1. Results from Models I and II

Although Model II simplifies the hydrodynamic behavior of bioreactor and algebraic and empirical equations are used, simultaneous prediction of phases and components dynamics including the effect of the biofilm growth in the fluidization characteristics during biological transients can be calculated. As an example, predicted values of the bed height and solid holdup for Models I and II are represented in Fig. 3.

Model II has the disadvantages of not predicting hydrodynamic transients and not reproducing non-ideal flow conditions when compared to Model I. The principal advantage of Model II is a lower numerical complexity because it is based on solution of ordinary differential equations (ODEs) (see Section 4).

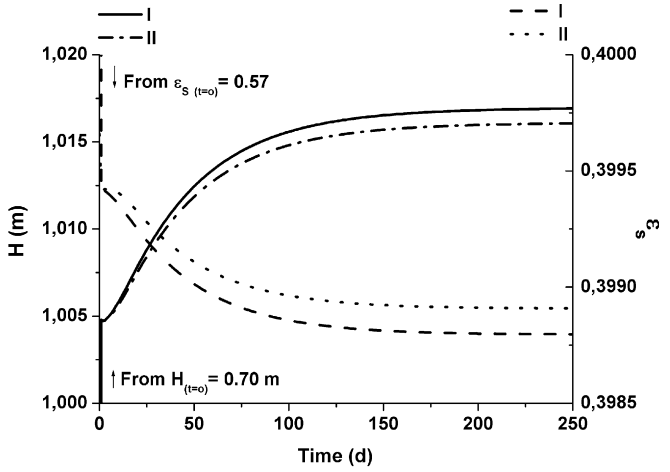

Fig. 3. Bed height (H) and solid holdup (ε_S) profiles predicted by Models I and II.

As expressed above, Model II allows to calculate dynamic variation of properties during a biological transient assuming a complete mixture behavior in all (three) phases. Fig. 4a and b show a comparison between predicted values of macroscopic variables: COD and biofilm concentration, and biogas flow rate and pH, respectively, for Models I and II.

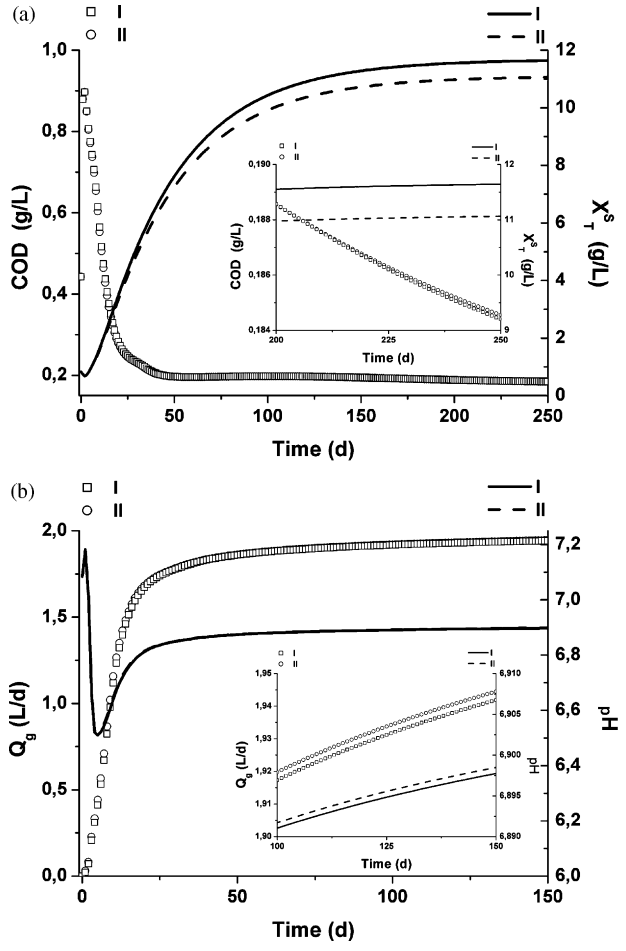

Fig. 4. Comparison of results from Models I and II: (a) COD and biofilm concentration (X^S_T) profiles, (b) biogas flow rate (Q_g) and pH profiles.

Biofilm concentration profiles differ in 5% (Fig. 4a). However, a deviation lower than 0.5% is obtained in the liquid and gas phase component concentrations. As observed in Fig. 4b, predicted values of system pH and biogas flow rate are almost the same for both modeling approaches. Therefore, practically the same COD removal efficiency is depicted by Models I and II.

3.2. Results from simplified models considering an incipient gas phase

For solving Model III, equation (7) is simplified and used to calculate the liquid phase dispersion coefficient ($D_{zL} = 0.04953\varepsilon_L U_L D_C^{1.66} d_{bp}^{-0.66}$). At the beginning of the biological transient, D_{zL} has the same value as in Model I, and a decrease of 0.21% is computed due to an increase of the biofilm concentration. A solid phase dispersion coefficient value equal to 10% of D_{zL} is used. These values assure uniform profiles in liquid and solid phases.

Fig. 5a and b show a comparison of results obtained from Models I and III. A decrease of 5.82% in biofilm concentration

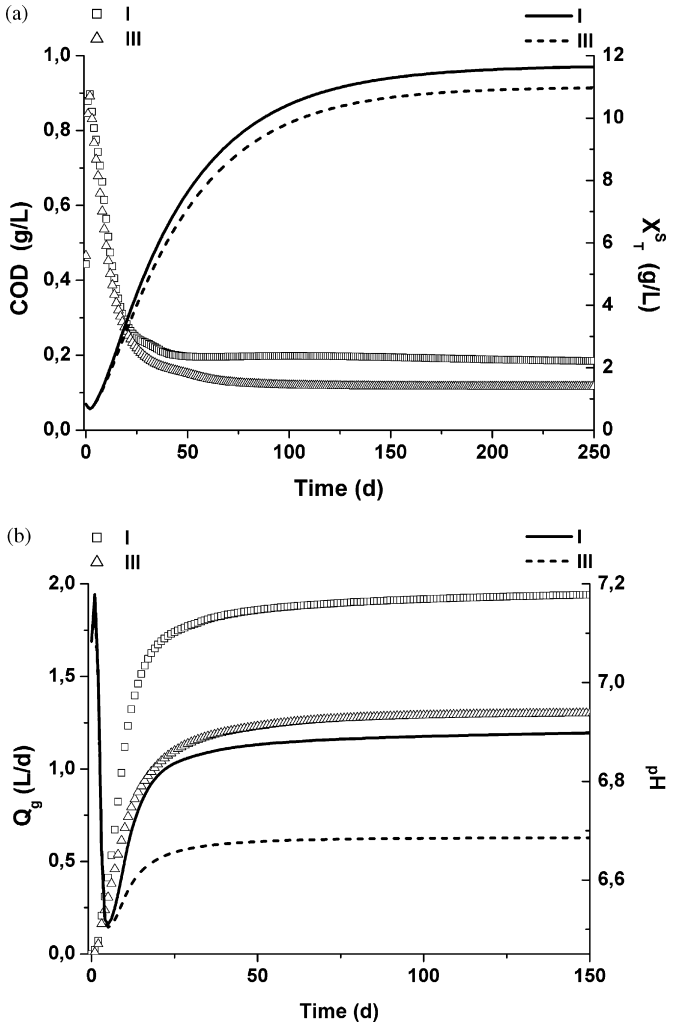

Fig. 5. Comparison of results from Models I and III: (a) COD and biofilm concentration (X^S_T) profiles, (b) biogas flow rate (Q_g) and pH profiles.

Table 4
Characteristics of AFBR models (I–IV)

Characteristic	Model I	Model II	Model III	Model IV
Prediction of transients	Hydrodynamic and biological	Biological	Hydrodynamic and biological	Biological
Phase flow conditions	Ideal and non-ideal flow	Ideal flow (complete mixture)	Ideal and non-ideal flow	Ideal flow (complete mixture)
Hydrodynamic system type	Three-phase S–L–G	Three-phase S–L–G	Two-phase S–L	Two-phase S–L
Numerical complexity	PDE (high index)	ODE (high index)	PDE (high index)	ODE (high index)
Equation number	3518	291	2959	258
Differential variable number	1045	52	990	52
CPU time (seconds)	>80[a]	<8	>80[a]	<8

[a] An additional programming effort to solve optimization and parameter estimation schedules are required.

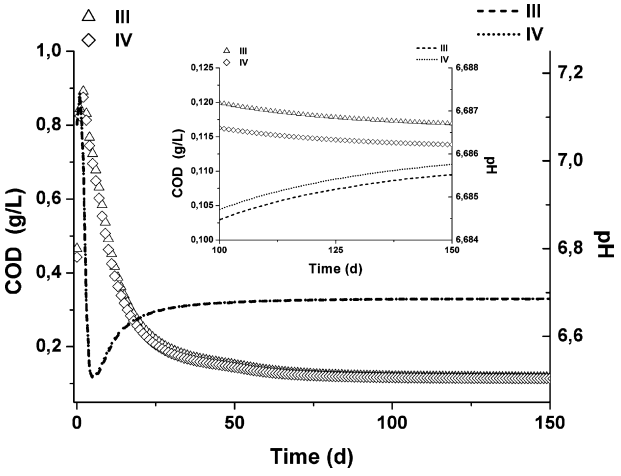

Fig. 6. Biofilm concentration (X_T^S) and pH profiles from Models III and IV.

is predicted by Model III, and total COD concentration values differ considerably (Fig. 5a). Contrarily to results from Model II, a high decrease in system pH values is obtained using Model III. It causes a decrease in the liquid–gas mass transfer rate and thus, in the biogas flow rate values (Fig. 5b).

As occurred with Model I and II, both simplified models (III and IV) present almost the same overall results. A difference of 1.3% in biofilm concentration steady state values is obtained between Models III and IV. Fig. 6 shows that there are almost no differences in system pH and COD profiles predicted by these modeling approaches.

From the above results, it is concluded that for the evaluated case study, ODE Models II and IV represent acceptably the totally dispersive flow condition calculated by PDE Models I and III, respectively.

4. Computational and numerical aspects

Different total COD removal efficiencies due to the ongoing microbiological and hydrodynamic processes were predicted by different AFBR models. Although these are theoretical results, simulation results show a trade-off between computational costs and precision at which bioreactor systems need to be modeled. Table 4 summarizes characteristics of all AFBR models.

Global AFBR Model I and its simplification for two-phase solid–liquid system, Model III, resulted in integral-partial derivative and algebraic equation (IPDAE) systems. On the other hand, Model II and its simplification, Model IV, are ordinary DAE systems. The implementation of AFBR models using gPROMS [8,9] makes the sensitivity analysis and simulation easier. From a numerical point of view, models (I and III) based on PDE solution are more complex and require a higher CPU time than the other ones based on ODE solution (Table 4). Backward finite difference method (BFDM) was used to solve PDEs. Using BFDM of second order over a uniform grid of 20 intervals, the total CPU time is about 80 s on an 800 MHz Pentium IV PC.

An additional programming effort was needed for all modeling aproaches since "high-index" DAE systems (index > 1) were verified. In high-index systems, the number of initial conditions that can be arbitrarily specified is lower than the number of differential variables; differential variables are not independent and numerical methods for solving ordinary differential equations can fail [9]. This problem can be solved by rewriting the derivative of some variables as functions of other differential variables, or directly assigning an initial condition for function to be integrated [1,2].

Models are able to resist strong numerical disturbances to represent a "step by step" start up of the bioreactor. gPROMS software includes modules for parameter estimation and optimization calculations. Models (I and III) based on PDE solution require an additional programming effort to implement estimation and optimization schedules. However, solutions are possible and more realistic operating schedules following non-ideal "real" flow patterns during biological and hydrodynamic transients can be investigated.

5. Conclusions

Results from four AFBR models were investigated attending to hydrodynamic flow conditions and the influence of gas phase on system hydrodynamics. Simulation results based on a case study allowed analyzing the bioreactor performance through the main variable profiles such as phase holdups and bed height, pH, COD, biofilm concentration and biogas flow rate. Based on the results obtained during this study, the following conclusions can be drawn:

1. All AFBR models simultaneously compute the dynamics of the phases and their components, including the effect of the biofilm growth in the fluidization characteristics. Models I and III, based on PDE solution, allow gathering predictions

in both hydrodynamic and biological transients, and ODE Models II and IV, only in biological transients.

2. For a case study based on a low organic concentration feed, the fact of considering a three-phase system with total developed flow (hydrodynamic pseudo-steady state) and complete mixture in all phases (Model II) causes deviations around 5 and 0.5% in predictions of biofilm concentration, and liquid and gas phase component concentrations, respectively. However, predicted total COD removal efficiency is almost the same for both models.
3. Although the gas holdup is negligible when compared with the liquid and solid ones in anaerobic fluidized bed reactors, results from model simplification assuming an incipient gas phase (Models III and IV) differ considerably with predictions from original three-phase modeling (Models I and II). A decrease in system pH values and thus, in biogas flow rate and COD removal efficiency of bioreactor are predicted.
4. As expressed above, the biological transient response calculated by the ODE Model II based on a hydrodynamic pseudo-steady state condition is very close to the totally dispersive flow condition calculated by the PDE Model I. A similar behavior was obtained when Models III and IV were compared. It seems to indicate that correlations used to calculate parameters and fluidization characteristics are reasonably well suited to predict the AFBR hydrodynamics. Since the biochemical and physico-chemical process rate equations are the same in all modeling approaches, the differences among results from Models I and II, and Models III and IV are settled by the simplifying assumption that reduces the three-phase gas–solid–liquid system to two-phase solid–liquid one, and neglects the gas phase contribution in reactor hydrodynamics.
5. From a computational point of view, three-phase ODE model (Model II) is an "inexpensive" variant to facilitate bioreactor performance analysis when operating conditions of reaction systems present a complete mixture behavior, which is characteristic of "high rate" fluidized bed reactors.
6. Since the system hydrodynamics is independent of the degradation stage number, AFBR models can be straightforward extended to different substrate degradation schemes. Prediction and reactor analysis of bioreactor configuration and hydraulic design are some practical applications for all AFBR models.

Acknowledgements

Financial support from Consejo Nacional de Investigaciones Científicas y Técnicas (CONICET), Agencia Nacional para la Promoción de la Ciencia y la Tecnología (ANPCyT) and Universidad Nacional del Litoral of Argentina is acknowledged.

Appendix A

A.1. Biochemical and physico-chemical processes

The anaerobic digestion model (ADM1, [7]) involves three enzymatic processes: (a) hydrolysis of undissolved carbohydrates, (b) of undissolved proteins, and (c) of undissolved lipids, and seven microorganism trophic groups: (1) glucose-fermenting acidogens, (2) amino acid-degrading acidogens, (3) long chain fatty acid (LCFA)-, (4) propionate-, and (5) butyrate and valerate-degrading acetogens, and finally (6) aceticlastic and (7) hydrogenotrophic methanogens.

Its application to a biofilm system requires the modeling of the interaction between suspended (X^{L}) and attached biomass (X^{S}). Main expressions for biochemical (uptake, growth, death, hydrolysis and detachment) process rates are summarized in Table A.1. A description of variables (i) and processes (j) involved in the anaerobic digestion model is presented in Table A.2.

Specific growth (μ) and death (k_d) rates are assumed to be the same for suspended and attached biomass. In addition, the specific biomass hydrolysis rate k_{bh} is the same for all species. Since non-active biomass is considered as particulate material subjected to disintegration and hydrolysis, k_{bh} is equal to the specific disintegration rate of particulate material k_{dis}.

The biofilm process model is coupled to the system hydrodynamic model through the biofilm detachment rate r_E which is modeled as a first-order function on the specific energy dissipation rate ω, and mass concentration of each attached microbial species i (Table A.1):

$$r_{E_i} = \varepsilon_S k_E \omega X_i^S \quad (A.1)$$

Specific energy dissipation rate ω was used by Huang and Wu [12] to study the biofilm thickness distribution in fluidized bed reactors, assuming that the erosion effects on the biofilm

Table A.1
Homogeneous reaction rates and mass transfer and transport process rates ($\sum_j R_{ik}^j + \sum_j T_{ik}^j$) involved in mass balance equations for component i [1,2]

ϕ_{ik}[a]	$\sum_j R_{ik}^j + \sum_j T_{ik}^j$	i
$X_{i_a}^S$	$\varepsilon_S[\mu_i X_{i_a}^S - k_{di} X_{i_a}^S - k_E \omega X_{i_a}^S]$	17–23
$X_{i_{na}}^S$	$\varepsilon_S[k_{di} X_{i_a}^S - k_{bh} X_{i_{na}}^S - k_E \omega X_{i_{na}}^S]$	17–23
$X_{i_a}^L$	$\varepsilon_L[\mu_i X_{i_a}^L - k_{di} X_{i_a}^L] + \varepsilon_S k_E \omega X_{i_a}^S$	17–23
$X_{i_{na}}^L$	$\varepsilon_L \left[k_{di} X_{i_a}^L - k_{bh} X_{i_{na}}^L\right] + \varepsilon_S k_E \omega X_{i_{na}}^S$	17–23
S_i	$\sum_{j=5-12} \nu_{i,j} \mu_j (\varepsilon_S X_{j_a}^S + \varepsilon_L X_{j_a}^L) + \sum_{j=2-4} \nu_{i,j} k_{Hid,j} \varepsilon_L X_j$	1–7, 11
S_i	$\sum_{j=5-12} \nu_{i,j} \mu_j (\varepsilon_S X_{j_a}^S + \varepsilon_L X_{j_a}^L) - \varepsilon_L (k_L a)_i (S_i - I_{COD} K_{H,i} p_{gas,i})$	8–10
X_i	$\sum_{j=2-4} \nu_{i,j} k_{Hid,j} \varepsilon_L X_j + \nu_{i,j=1} k_{dis} \varepsilon_L X_C$	12, 14–16, 24
X_C	$-k_{dis} \varepsilon_L X_C + k_{dis} \sum_{j=13-19} (\varepsilon_S X_{j_{na}}^S + \varepsilon_L X_{j_{na}}^L)$	13
$P_{gas,i}$	$\nu_{st} p_{gas,T} \varepsilon_L (k_L a)_i (S_i / I_{COD} - K_{H,i} p_{gas,i})$	8–10

[a] Mass balances of phase components are expressed in grams of chemical oxygen demand per liter per day (g COD L^{-1} d^{-1}), except for inorganic carbon and nitrogen (mol L^{-1} d^{-1}) and gas phase components (atm L^{-1} d^{-1}).

Table A.2
Variables (*i*) and processes (*j*) taken into account in the anaerobic digestion model [1,2]

Variable	Description	*i*	Processes	*j*
X_C	Composite	13	Disintegration	1
X_{CH}	Carbohydrate	14	Carbohydrate hydrolysis	2
X_P	Protein	15	Protein hydrolysis	3
X_{Li}	Lipid	16	Lipid hydrolysis	4
X_I	Inert particulate	24	Glucose uptake	5
S_I	Inert soluble	12	Amino acid uptake	6
S_{GI}	Glucose	1	LCFA uptake	7
S_{AA}	Amino acid	2	Valerate uptake	8
S_{LCFA}	LCFA	3	Butyrate uptake	9
S_{HVa}	Valerate	4	Propionate uptake	10
S_{HBu}	Butyrate	5	Acetate uptake	11
S_{HPr}	Propionate	6	H_2 uptake	12
S_{HAc}	Acetate	7	X_{GL} decay	13
S_{H_2}	Hydrogen	8	X_{AA} decay	14
S_{CH_4}	Methane	9	X_{LCFA} decay	15
S_{IC}	Inorganic carbon	10	X_{C4} decay	16
S_{IN}	Inorganic nitrogen	11	X_{Pr} decay	17
X	Biomass	17–23	X_{Ac} decay	18
			X_{H_2} decay	19
			H_2 mass transfer	T8
			CH_4 mass transfer	T9
			CO_2 mass transfer	T10

surface are related to this parameter that is calculated as:

$$\omega = U_0 \left(-\frac{\partial p}{\partial z} \right) \tag{A.2}$$

Specific detachment rate k_E is assumed to be the same for all biological species [1,2].

ADM1 assumes H_2, CO_2 and CH_4 as components of the gas phase. Here, water vapor has been considered too. The liquid–gas mass transfer is modeled assuming ideal gas behavior, and gas phase total pressure constant. The mass balance for gas phase component *i* is expressed as a function of its partial pressure $p_{gas,i}$ (Table A.1). Water vapor pressure is calculated by an Antoine-type equation.

The physico-chemical model includes the system charge balance (electroneutrality condition) for calculating pH. It involves mass balance equations for total concentration of volatile fatty acids (VFAs: acetic, propionic, butyric and valeric), inorganic carbon, inorganic nitrogen, phosphate, "other anions", and "other cations".

The biochemical rate equation matrix, the relationships of the acid–base equilibrium model, and kinetic and physico-chemical parameters (at mesophilic and high rate operating conditions) are extracted from Batstone et al. [7,2].

Appendix B. Nomenclature

A area
C_D drag coefficient
D, d diameter
D_z axial dispersion coefficient
F force
g gravity
H height
I_{COD} index (g COD mol^{-1})
k specific rate coefficient, GBWM parameter (Table 2)
k_La liquid–gas mass transfer coefficient
K_H Henry's coefficient
n expansion coefficient
N number
P, p pressure
Q flow rate
R homogeneous reaction rate
Re Reynolds number
S soluble species concentration
T mass transfer and transport process rate at the interface
t time
U velocity
V volume
W particle load
X biomass concentration or non-soluble species concentration
X_c particulate material concentration
z axial direction

Greek letters
δ biofilm thickness
ε holdup (volumetric fraction)
μ specific growth rate (Table A.1), viscosity
ν_{st} gas molar volume
ξ holdup in two-phase pseudo-system
ρ density
ω specific energy dissipation rate
ϕ mass or molar concentration
- axial mean value

Subscripts
a active (biomass)
bh biomass hydrolysis
bp bioparticle
c reactor column
d biomass death
dis disintegration of particulate material
E biofilm detachment
Es relative to the force acting on fluidized particles in the axial direction
F film (wet density)
f feed
G, g gas, gravity (force)
H particulate material hydrolysis
I interaction (force)
i phase component index
in inlet
j biochemical and physico-chemical process index
k phase index
L, l liquid
na non-active (biomass)
out outlet
p particle, pressure (force)

r recycle
S solid
t terminal

References

[1] M. Fuentes, M.C. Mussati, N.J. Scenna, P.A. Aguirre, Global modeling and simulation of a three-phase fluidized bed bioreactor, Comput. Chem. Eng., Ms. Ref. No.: 4281, submitted for publication.

[2] M. Fuentes, Modeling and dynamic simulation of anaerobic biofilm fluidized bed reactors. Application to the complex effluent treatment, Ph.D. dissertation (in Spanish, ISBN-10: 987-05-0709-3, ISBN-13: 978-987-05-0709-3), Universidad Nacional del Litoral, Santa Fe, Argentina, 2006.

[3] B. Bonnet, D. Dochain, J.P. Steyer, Dynamical modelling of an anaerobic digestion fluidized bed reactor, Water Sci. Technol. 36 (5) (1997) 285–292.

[4] Z. Chen, L.G. Gilibaro, P.U. Foscolo, Two-dimensional voidage waves in fluidized beds, Ind. Eng. Chem. Res. 38 (1999) 610–620.

[5] N. Hatta, H. Fujimoto, M. Isobe, J. Kang, Theorical analysis of flow characteristics of multiphase mixtures in a vertical pipe, Int. J. Multiphase Flow 24 (4) (1998) 539–561.

[6] S. Talvy, A. Cockx, A. Line, Global modeling of a gas-liquid-solid airlift reactor, Chem. Eng. Sci. 60 (2005) 5991–6003.

[7] D.J. Batstone, J. Keller, I. Angelidaki, S.V. Kalyuzhnyi, S.G. Pavlostathis, A. Rozzi, W.T.M. Sanders, H. Siegrist, V.A. Vavilin, Anaerobic Digestion Model No. 1 (ADM1), IWA Task Group for Mathematical Modelling of Anaerobic Digestion Processes., IWA Publishing, London, UK, 2002.

[8] Process Systems Enterprise Ltd., gPROMS Advanced User Guide, Release 2.3, London, 2004.

[9] Process Systems Enterprise Ltd., gPROMS Introductory User Guide, Release 2.3.1, London, 2004.

[10] M.A. Abdul-Aziz, S.R. Asokelar, Modeling of biological particle mixing in a fluidized-bed biofilm reactor, Water Environ. Res. 72 (2000) 105–115.

[11] V. Diez Blanco, P.A. García Encina, F. Fdez-Polanco, Effects of biofilm growth, gas and liquid velocities on the expansion of an anaerobic fluidized bed reactor (AFBR), Water Res. 29 (7) (1995) 1649–1654.

[12] J. Huang, C. Wu, Specific energy dissipation rate for fluidized bed bioreactors, Biotechnol. Bioeng. 50 (1996) 643–654.

[13] J. Huang, J. Yan, C. Wu, Comparative bioparticle and hydrodynamic characteristics of conventional and tapered anaerobic fluidized-bed bioreactors, J. Chem. Technol. Biotechnol. 75 (2000) 269–278.

[14] K. Muroyama, L.S. Fan, Fundamentals of gas-liquid-solid fluidization, AICHE J. 31 (1985) 1–34.

[15] V.K. Bhatia, N. Epstein, Three-phase fluidization: a generalized wake model, in: Proceedings of the International Syrup. Fluid. Appl., Cepadues-Editions, Toulouse, 1974, pp. 380–392.

[16] J.F. Richardson, W.N. Zaki, Sedimentation and fluidization, Part 1, Trans. Inst. Chem. Eng. 32 (1954) 35–53.

[17] G.I. Efremov, I.A. Vakhrushev, A study of the hydrodynamics of three-phase fluidized beds, Int. Chem. Eng. 10 (1970) 37–41.

[18] H. Yu, B.E. Rittmann, Predicting bed expansion and phase holdups for three-phase fluidized-bed reactors with and without biofilm, Water Res. 31 (10) (1997) 2604–2616.

[19] S.H. Chern, L.S. Fan, K. Muroyama, Hydrodynamics of concurrent gas–liquid–solid semifluidization with a liquid as the continuous phase, AICHE J. 30 (1984) 288–294.

[20] T. Miyahara, L.S. Fan, Properties of a large bubble in a bubble swarm in a three-phase fluidized bed, J. Chem. Eng. Jpn. 25 (1992) 378–382.

[21] S.W. Hermanowicz, J.J. Ganzarczyk, Some fluidization characteristics of biological beds, Biotechnol. Bioeng. 25 (1983) 1321–1330.

[22] L.T. Mulcahy, W.K. Shieh, Fluidization and reactor biomass characteristics of the denitrification fluidized bed biofilm reactor, Water Res. 21 (1987) 451–458.

[23] K.-F. Ngian, W.B. Martin, Bed expansion characteristics of liquid fluidized particles with attached microbial growth, Biotechnol. Bioeng. 22 (1980) 1843–1856.

[24] T. Setiadi, Predicting the bed expansion of an anaerobic fluidized bed bioreactor, Water Sci. Technol. 31 (1995) 181–191.

[25] C.R. Thomas, J.G. Yates, Expansion index for biological fluidized beds, J. Inst. Chem. Eng. 63 (1985) 67–70.

[26] P.U. Foscolo, L.G. Gilibaro, S.P. Waldarm, A unified model for particulate expansion of fluidized beds and flow in fixed porous media, Chem. Eng. Sci. 38 (8) (1983) 1251–1260.

[27] R.H. Perry, C.H. Chilton, Chemical Engineer's Handbook, fifth ed., McGraw-Hill, New York, 1973.

[28] W.K. Shieh, C.Y. Chen, Biomass hold-up correlations for fluidized bed biofilm reactors, J. Chem. Eng. Res. Des. 62 (1984) 133–136.

[29] M. Mussati, C. Thompson, M. Fuentes, P. Aguirre, N. Scenna, Characteristics of a methanogenic biofilm on sand particles in a fluidized bed reactor, Lat. Am. App. Res. 35 (2005) 265–272.

[30] M. Fuentes, P.A. Aguirre, N.J. Scenna, M.C. Mussati, Anaerobic biofilm reactor modeling focused on hydrodynamics. Chem. Eng. Commun. (2007), in press.

[31] S.D. Kim, C.H. Kim, Axial dispersion characteristics of three phase fluidized beds, J. Chem. Eng. Jpn. 16 (1983) 172–178.